TFAST project - Description of the main S & T results

Consortium consists of 16 partners:

No	Participant name	Short	Conutry	EXP	CFD
1	INSTYTUT MASZYN PRZEPLYWOWYCH IM ROBERTA SZEWALSKIEGO POLSKIEJ AKADEMII NAUK - IMP PAN	IMP	Poland	X	X
2	ROLLS-ROYCE DEUTSCHLAND LTD & CO KG	RRD	Germany		X
3	DASSAULT AVIATION SA	DAAV	France		X
4	CENTRE NATIONAL DE LA RECHERCHE SCIENTIFIQUE (UNIVERSITE D'AIX MARSEILLE)	IUSTI	France	X	X
5	OFFICE NATIONAL D'ETUDES ET DE RECHERCHES AEROSPATIALES (DAFE, DAAP)	ONERA	France	X	X
6	DEUTSCHES ZENTRUM FUER LUFT - UND RAUMFAHRT EV (Koeln, Goettingen)	DLR	Germany	X	
7	NUMERICAL MECHANICS APPLICATIONS INTERNATIONAL SA	NUMECA	Belgium		X
8	INSTYTUT LOTNICTWA	IoA	Poland	X	X
9	KHRISTIANOVICH INSTITUTE OF THEORETICAL AND APPLIED MECHANICS OF SIBERIAN BRANCH OF RUSSIAN ACADEMY OF SCIENCE	ITAM	Russia	X	
10	THE CHANCELLOR, MASTERS AND SCHOLARS OF THE UNIVERSITY OF CAMBRIDGE	UCAM	UK	X	
11	TECHNISCHE UNIVERSITEIT DELFT	TUD	Netherlands	X	
12	UNIVERSITY OF SOUTHAMPTON	SOTON	UK		X
13	UNIVERSITA DEGLI STUDI DI ROMA LA SAPIENZA	URMLS	Italy		X
14	THE UNIVERSITY OF LIVERPOOL	LIV	UK		X
15	INSTITUT NATIONAL POLYTECHNIQUE DE TOULOUSE	IMFT	France		X
16	THE PODGORNY INSTITUTE FOR MECHANICAL	UAN	Ukraine		X

TFAST projects consists of 5 work packages:

Work Package 1 (WP-1) - Reference cases of laminar and turbulent interactions (Leader: IUSTI)
Work Package 2 (WP-2) - Basic investigation of transition effect (Leader: UCAM)
Work Package 3 (WP-3) - Internal flows – compressors (Leader: RRD)
Work Package 4 (WP-4) - Internal flows – turbine (Leader: DLR)
Work Package 5 (WP-5) - External flows – wing (Leader: DAAV)

The basic research in WP-1 and WP-2 is closely related to three Work Packages concerning technical applications where the location of transition is a dominant issue in their further improvement of performance. These technical cases concern: flow in transonic compressor cascade (WP-3), high pressure turbine cascade with cooling system (WP-4) and a transonic laminar wing (WP-5).

Work Package 1 - Reference cases of laminar and turbulent interactions

Work package tasks – partnership and sharing of work

Two main configurations have been studied: the Oblique Shock Wave Reflection and the Normal Shock Wave. Mach numbers ranging from 1.45 to 1.7 were considered for the OSWR while a single Mach number of 1.2 was considered for the NSW. The different configurations have been distributed among the eight partners involved in this work package:

Table 1: WP-1 partners and investigated cases

Partner	Location	Flow	Mach	contribution
ITAM	Novosibirsk, Russia	OSWR	1.45	EXP
IUSTI	Marseille, France	OSWR	1.6	EXP / CFD
ONERA	Meudon, France	OSWR / NSW	1.6 / 1.2	EXP / CFD
TUD	Delft, Netherlands	OSWR	1.7	EXP
UCAM	Cambridge, UK	NSW	1.2	EXP
IMFT	Toulouse, France	OSWR	1.7	CFF
SOTON	Southampton, UK	OSWR	1.5	CFD
URMLS	Rome , Italy	NSW	1.2-1.3	CFD

The technical specificities of the different wind tunnels cover a wide range of unit Reynolds number ($5 \cdot 10^6$ to $35 \cdot 10^6$) and of initial perturbations (external pressure perturbations from 0.4 to 2%).

Three tasks were defined:

1.1. Test section design and construction
1.2. Fully laminar interaction
1.3. Fully turbulent interaction

The task 1.2 was the most challenging as no recent experimental set-up were available at the beginning of the program. Several wind tunnel breakdowns occurred during the project (UCAM, ONERA, TUD, IUSTI). The more serious problem occurred at IUSTI with a problem on the compressor of the wind tunnel. This delayed the restart of the experiments to the second quarter of 2012, two years after the beginning of the project. This reduced considerably the time to complete experiments and obliged to perform *blind numerical simulations*, as no experimental conditions were available on time.

All experimental partners succeeded in developing operational set-ups for the OSWR. It should be noted that highly stable and repeatable experimental conditions have been obtained, allowing cross comparisons between several metrologies and experiments. Laminar to turbulent upstream conditions have been obtained, documented and used for numerical simulations

Partners involved in the NSW configuration have experienced serious experimental worries. None was able to obtain stable laminar NSW interactions for such low Mach number, with upstream laminar flow with a plate sharp leading edge . UCAM succeeded to obtain a stable configuration using an elliptical leading edge.

The experimental partners used a wide range of methods: Schlieren (in some cases time resolved), hot wire, Pitot probes, high spatial resolution LDA and PIV, Pressure and Temperature Sensitive Paints, unsteady wall pressure sensors.

In parallel, a wide panel of numerical simulations has been used: 2D URANS, DDESs, 3D LES and DNS. LES and DNS results confirm the experimental observations: the transitional interactions are unsteady (low frequencies) and separated, and the turbulent one are attached and steady. SOTON develops multimodal LST analysis, with forcing at the inflow, based on the ONERA and ITAM configurations.

Conclusions from WP-1 Partners

All partners obtained upstream laminar conditions following theoretical laminar boundary layer properties. Transition of the boundary layer was obtained for Reynolds number around 2.10^6 (IUSTI did not obtain natural transition along the plate). For the highest possible total pressure in IUSTI facility, transition begins close to the trailing edge of the plate, which corresponds to a Reynolds number of $2{\cdot}10^6$).

A particular effort has been made to evaluate the onset of separation of the laminar boundary layer. The direct evaluation was difficult due to blockage effects for very low flow deviations. TU-Delft observed marginal flow separation for imposed flow deviation as low as 1°. The onset of separation has been studied from the IUSTI Large Eddy Simulations. These simulations have shown that a flow deviation as small as 1° flow deviation was sufficient to obtain an incipient interaction. This is consistent with empirical relations based upon the free-interaction theory: this validation, provided comparisons between the considered OSWI. When turbulent upstream conditions are considered, no separation is observed, whatever the flow deviation. Beyond 5° (or less for lower Mach numbers) turbulent OSWI induces Mach stems.

The length scales of the interaction have been derived for all configurations. In case of the OSWR, dependences on the imposed flow deviation, unit Reynolds number and upstream level of perturbations have been documented. Large differences between experimental results have been obtained concerning the resulting aspect ratio (L/δ_0, with L the interaction length and δ_0 the displacement thickness of the natural boundary layer at the onset of the interaction): they can differ by more than 100% between the different partners. The influence on the mean field of the upstream unsteadiness has been described in details from IUSTI's experiments and LES and from ITAM's experiments. Combining natural transition and tripped upstream boundary layer (keeping a laminar upstream flow, see WP2 results for more details), these large differences on the aspect ratio of the interaction have been explained by the upstream level perturbations, which may differ significantly between the different experimental facilities. Therefore, only qualitative comparisons were achieved with the transitional experiments. Quantitative comparisons between simulations and experiments would require adjusting the amplitude of disturbances in the upstream boundary layer in order to obtain the same length of interaction. It has to be pointed out that in this case the simulations are no more predictive. The capability to predict accurately the length of interaction if the input perturbation are known (size, amplitude, space-time properties) remains an open question. For the turbulent cases, LES and DNS numerical simulations compared well with experiments from TU-Delft, IUSTI and UCAM if main characteristic properties of the downstream flow are considered (displacement and momentum thicknesses, shape factor, friction coefficient C_f).

The geometrical properties of the interaction (length of interaction, reattachment location, transition location) have been documented from all partners, using different methods. In general, no fully laminar interaction is experimentally observed. Transition occurs always inside the interaction. ONERA and TU-Delft showed that for small flow deviation and/or reduced unit Reynolds number, transition is observed slightly downstream from the impingement location. When flow deviation and/or unit Reynolds number are increased, transition occurs just downstream of the shock impingement and the flow is reattaching. The reversed region shares some characteristic features with the *Free Interaction Theory*. IUSTI's experiments and LES and TU-Delft's experiments have shown that the initial part of the separation region does not depend on the imposed deviation. Constant pressure rises as well as flow deviation (of about 2°) have been observed for all cases and the separation bubbles have been found homothetic for a wide range of shock intensities.

Whatever the geometry (OSWR or NSW), the downstream conditions are always turbulent (or nearly turbulent): the interaction can be considered as an effective tripping system for the transition to turbulence for the upstream laminar boundary layer. The downstream mean field relaxes quickly to fully turbulent conditions. As for turbulent interactions, the turbulent fields relax significantly more slowly than the mean fields.

Unfortunately, the turbulent fields have been less documented, because of the extreme experimental conditions. ITAM (micro-PIV) and IUSTI (38µm LDA) provided turbulent fields along the interaction. The transitional evolution of the mixing layer, which is developing over the separated region, has been documented. Experimental and numerical IUSTI results showed that the transition of the mixing layer, characterized by a saturation level of the velocity fluctuations amplitudes, defines the reattachment of the flow.

Significant efforts have been carried out to obtain experimental descriptions of the unsteadiness along the interaction. This point was not a centrepiece of the TFAST program. Nevertheless, a large dependence of the mean field on the amplitude of the upstream unsteadiness has been demonstrated during the project which required to document this point in more details as initially planned.

Experiments from IUSTI, ITAM and ONERA shown that the considered transitional OSWR were unsteady, with evidences of low frequencies, which are about one order of magnitude lower than the characteristic unsteadiness observed in the laminar boundary layer from unsteady hot wire measurements. IUSTI provided extensive results concerning the longitudinal evolution of these unsteadiness for various upstream conditions and flow deviation angles. The unsteadiness developing inside the interaction involves lower frequencies than those observed in the upstream laminar boundary. Non-dimensional frequencies (Strouhal numbers) have been estimated: some controversy remains between the different results. IUSTI and SOTON simulations suggest Strouhal numbers about 0.04 and 0.5 for the low frequencies and mixing-layer frequencies, respectively, as in separated turbulent interaction. On the opposite, IUSTI experiments suggest values of respectively 0.12 and 0.5, when ONERA simulations propose intermediate values of 0.09. If all partners observed evidences of low frequency unsteadiness in transitional interactions, the accurate estimation (and of course the origin) of the unsteadiness remains an open question. Numerical results (IUSTI, ONERA, SOTON) showed that the low frequencies are associated with negative convection velocity: a Fourier analysis would suggest that they are generated in vicinity of the reattachment region and propagate in the upstream direction. Unfortunately, no phase information was available from the experiments during the project. A surprising result came from IUSTI experiments and numerical simulations: for a fixed flow deviation, the amplitude of the low frequency unsteadiness has been found to vary as the aspect ratio of the interaction. Shorter is the interaction (i.e. larger the upstream perturbations) higher are their amplitudes.

Finally, as already mentioned, transition to turbulence is observed at reattachment, and large energetic structures are shed downstream of the interaction as in turbulent separated interaction. Therefore, the turbulent field remains out of equilibrium downstream from the reattachment, being possibly an issue for the modelling of this region.

Recommendations for future work and for practical applications

These results of course have strong consequences for the aeronautical applications. Transitional interactions have been proved to be an efficient way to promote transition to turbulence downstream from the interaction. Nevertheless, special care must be taken regarding the low and high frequency unsteadiness developed in separated interactions. These unsteadiness have been shown to have a large influence on the mean field of the interaction. Now, the elements and the expertise for a more detailed analysis of the unsteadiness of such flows, their origin and their precise characterization are available.

It is recommended also to analyse the “turbulent” field formed downstream of the interactions, and to focus on such conditions in the future, to test current modelling. Turbulence generated in such conditions is very particular, and has probably not yet reached asymptotic properties. This has to be described experimentally, and their modelling will require probably non standard adaptations.

In aeronautical situations, the consequence is that the effort should be put on the definition of the perturbations upstream of the interactions. This depends of course on each particular case, but advanced engineering methods can investigate this point: this is the key issue for the prediction of

such flows. A last recommendation can be made: it would be probably useful to use advanced modelling like LES or even DNS in some cases, to calibrate simpler and cheaper models of handy use for current design.

Work Package 2 - Basic investigation of transition effect

Work package tasks – partnership and sharing of work

Table 2 lists the partners involved in WP2 and the flow control devices investigated. It can be seen that the research covered a wide range of devices from traditional 'mechanical' transition trips to more complex active controls. In each case the partners used the same facilities and flow configurations as described in WP1. Therefore the methodologies will not be repeated here.

Typically, transition control devices were placed at Reynolds numbers (based on streamwise distance from the origin of the boundary layer) of $1.5 \cdot 10^5$ to $7 \cdot 10^6$. Mostly, devices were located at Reynolds numbers in the range of $5 \cdot 10^5$ to $1.5 \cdot 10^6$. Each devices was tested in a variety of sizes or strengths, as shown in Table 3.

Table 2: WP-2 partners and flow control devices investigated

	2D mechanical		**3D**		**VG**		**Plasma**
	Roughness	Step	Zig-zag	Dots	rod-VG	Air-jet	
IUSTI		X					
ONERA			X	X		X	
ITAM		X					X
UCAM		X		X			
TUD	X	X	X				
SOTON							X
URMLS					X		
IoA						X	

Table 3: Control devices and relative height
(expressed in local boundary-layer thickness) or 'strength' (expressed in local flow momentum)

Device type	**Size or 'Strength'**
Roughness	3-10% of δ
Step, Zig-zag tape	10-130% of δ
Dots	10% of δ to $\gg \delta$
Vortex generators (mechanical)	δ to several δ
Air-jet vortex generator	20-60% of U_∞
Plasma	<5% of U_∞

The research was broken down into two subtasks:

Task-2.1 Study of operation of transition control devices

In this sub-task the effectiveness of control devices to trigger transition ahead of the shock wave was investigated. Broadly speaking, it was observed that all mechanical devices triggered transition successfully. The only exceptions were very small devices applied in facilities with very low free-stream Reynolds numbers. Any device with a device-height Reynolds number of 1000 or greater was found to triggered transition. In fact, the relatively small device height required for transition tripping resulted in most devices under study being considerably larger than necessary. Indeed, many partners reported evidence of 'over-tripping'. The main symptom of this was a rapid boundary-layer growth across the device, leading to the flow downstream of such devices featuring a thicker boundary layer than that observed in natural (free) transition.

For the 'momentum' devices it was observed that a minimum of around 20% of 'free-stream momentum is necessary to successfully trip the boundary layer to turbulence. Consequently, plasma devices were unable to promote turbulence (as seen in Table 3, their strength was well below this level). A 'hypothetical' numerical study at SOTON investigated (as yet unfeasible) plasma devices at greater strength and here transition was observed when the plasma-induced jet velocity exceeded approximately 20% of the local free stream.

Task-2.2 Interaction sensitivity to transition location

In this task the effect of artificially tripping the boundary layer ahead of a shock on the shock wave / boundary layer interaction was studied.

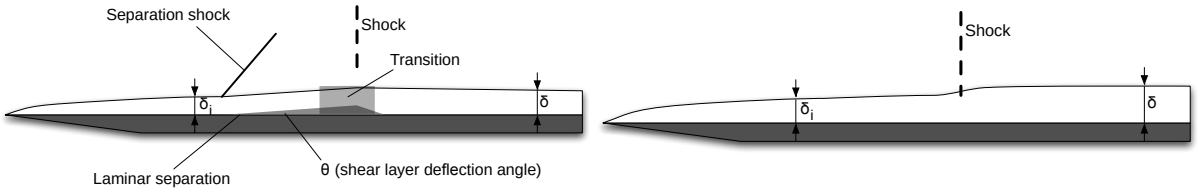

Fig. 1 Schematic view of a) laminar separation bubble caused by shock-induced pressure rise and, b) turbulent or tripped interaction (no separation)

The majority of research groups noted no fundamental difference in the overall flowfield between the tripped and untripped flows. While laminar flow ahead of the shock wave generally led to the existence of a laminar separation, the common observation was that this very quickly caused transition and turbulent re-attachment in the vicinity of the main shock wave as illustrated schematically in Fig.1a. When the flow was tripped ahead of the shock (or transitioned naturally to turbulence) no laminar separation was seen, as expected (see Fig. 1b). In all cases the flow downstream of the SBLI appeared relatively similar, whether it had transitioned inside a laminar separation bubble or ahead of the interaction, suggesting that there were no adverse effects caused by the existence of a laminar separation. In fact, the most common observation was that tripped flows exhibited thicker boundary layers (due to over-tripping) across and downstream of the interaction, suggesting that in such cases the effects of tripping were predominantly unfavourable.

This raises the question why a laminar separation bubble is seen as a relatively benign event. The answer to this lies in the fact that the pressure rise at separation is very small for laminar boundary layers. Thus, the pressure jump at the separation point (and thus the strength of the separation shock wave) is very small and the flow deflection angle θ (formed by the separating shear layer and the wall) is also very small (of the order of 1°). Hence, although laminar separations are typically quite long (the separation location is many boundary layer thicknesses upstream of the shock wave) the height of such separations remains quite small. Therefore, the existence of a laminar separation causes negligible effects on the outer flow because the associated shock wave is vanishingly weak and the displacement of the boundary layer edge is very small. Following separation, the instability of the separated shear layer makes this very prone to transition. Thus,

transition is observed either upstream of the main shock or, at the latest, underneath the main shock wave where the additional pressure pulse leads to a very quick transition and subsequent flow re-attachment as seen in Fig.1a.

Consequently, the boundary layer thickness δ downstream of the interaction is often smaller than that observed in a turbulent or tripped interaction where the incoming boundary layer δ_i may be significantly thicker than in the laminar case.

This finding is illustrated by Fig.2 which shows the development of boundary layer thickness and shape factor across and downstream of a normal SBLI, comparing 'clean' cases (laminar inflow) with various tripped cases. It can be seen that, despite the fact that the laminar cases featured a separated interaction, there are no fundamental differences in the post-interaction boundary layer development. In fact, it can be seen that the 'clean' flow cases experienced a faster recovery to typical equilibrium shape factors and a slightly reduced boundary layer thickness compared to tripped cases.

These findings were common to all partners of WP-2. Most groups concluded that for the flow configurations under study, namely flat plate interactions of normal and oblique shock waves, there was no benefit in tripping the flow ahead of the shock wave. Given that most trips exhibited evidence of over-tripping the recommendation is thus to avoid tripping altogether for such geometries.

Flow unsteadiness was rarely found to be affected by the presence of laminar separation. The only flow scenario where unsteadiness was enhanced was reported by IUSTI for the case of tripped flows. Thus, it was once again concluded that it allowing the interaction to trigger turbulence is not detrimental.

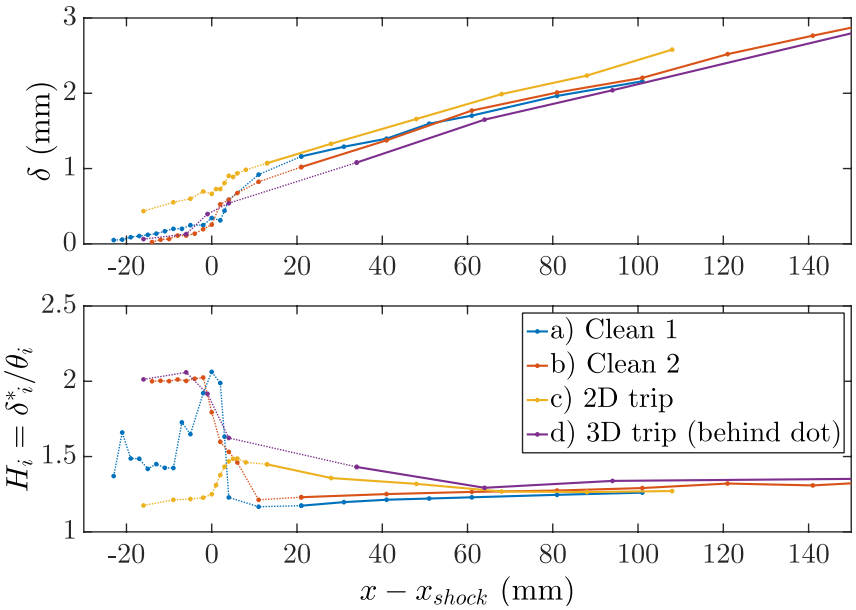

Fig. 2 Boundary layer properties across a normal SBLI, comparing 'Clean' (natural transition in SBLI region) and tripped cases. Despite being separated, 'clean' cases exhibit faster recovery and thinner boundary layers downstream of the interaction (UCAM)

Conclusions from WP-2 Partners

The main conclusions of this work package can be summarised as follows:

- Most mechanical tripping devices were successful at promoting turbulent flow, except for very small devices (below Re_H=1000 at low Re).
- 'Active devices' (air-jet VGs or plasma) needed a minimum 'strength' to successfully promote transition. This is roughly of the order of 20% of free stream flow momentum. Plasma devices are currently unable to reach this level of 'strength' in high-speed flows.

- Most devices caused over-tripping, leading to thicker (and less full) boundary-layers post-shock compared to natural transition.
- When the flow was left to transitional naturally in the SBLI region, the most commonly observed flowfield featured a laminar separation followed by transition in the vicinity of the shock and turbulent re-attachment. Despite the fact that clear differences in the flow were observed at a local level, the global flowfield was not fundamentally different from an attached turbulent interaction. This included flowfield unsteadiness. Thus, it can be concluded that in many cases a laminar separation does not significantly alter the outer flow or cause any long-term damage to the boundary-layer flow across and downstream of the interaction.

Work Package 3 - Internal flows – compressors

Work package tasks – partnership and sharing of work

In order to have deeper insight to the compressor cascade application two test facilities are used. One for a basic study which allows a deeper insight into the interaction flow details. It is a single passage test section representative for the flow conditions in real cascade. The experimental and numerical investigations were carried out at IMP PAN within Task 3.1 (*Single passage test section*). The second test section is a linear cascade, built and investigated at DLR in Köln. The experimental and numerical investigations for cascade configuration were split into two tasks: Task 3.2 *Compressor cascade basic flow* and Task 3.3 *Compressor cascade flow with transition control.* It is necessary to highlight few aspects of transonic compressor test section that make investigations very demanding in single passage test section. The profile defined by industrial partner RRD is representative for an in-service fan blade section. It appeared a very challenging aerodynamic duty to fulfil inlet Mach number=1.22, flow deflection angle=15 degrees and AVDR =1.2 (axial Velocity Density Ratio) in a single passage configuration. The influence of stream tube contraction, typically expressed with AVDR parameter, and particularly short spans to chord ratios of the test section, both promoting flow separation and strong main and end-wall flow interactions, that resulted in unexpected increase in effort, which was required to get the test section designed. Finally, the system of suction slots at wind tunnel walls was designed and the required conditions were obtained (Fig. 3). Test section was designed by means of numerical simulations at IMP PAN and CFD predictions by NUMECA.

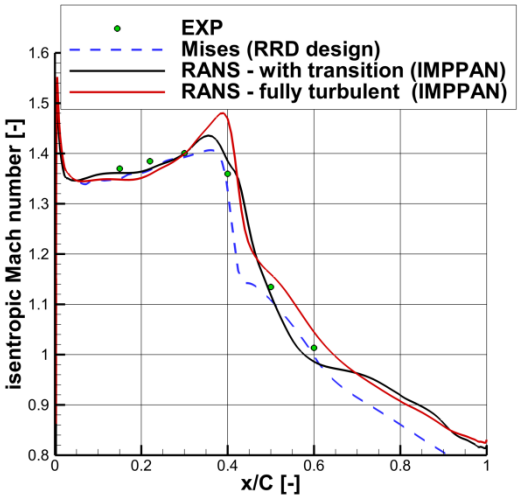

Fig. 3 Isentropic Mach number on the suction side

Table 4: Roughness patch locations and Ra [μm]

x/c=0.11	x/c=0.16	x/c=0.22
12	20	20
10	16	16
8	12	12
	10	10
Strip width 10 mm	Strip width 5 mm	Strip width 5 mm

In case of cascade configuration (DLR), an extensive numerical investigation of the bleed slot location effect on AVDR and the sensitivity of the sucked mass flow was done by RRD and NUMECA (task. 3.2). Due to the complexity of the end wall flows, uncertainties of URANS predictability of those flows and possible negative interactions in respect to flow visualisation in the experiment, the proposed suction slot design of DLR was chosen finally.

In task 3.1, for reference (laminar interaction) and transition flow cases the following measurements are carried out: static pressure along the lower wall and blade, schlieren and oil visualization, PSP and TSP (Pressure and Temperature Sensitive Paint), shock oscillations measurements, velocity traverses (LDA measurements) of the upstream profile and in the wake. Transition was induced by three methods:

- strip: 3 locations: at leading edge and x/c = 0.16; 0.22,
  3 step heights: 50, 100, 400 μm
- roughness patch (Tab. 4)
- Air Jet Vortex Generators: hole diameter D 0.3 mm (~ boundary layer thickness) , pitch angle ϕ=30° and skew angle θ=90°, spanwise distance L/D=15

Based on the results of investigations in single passage test section (task 3.1), the transition control cases were defined and investigated in DLR cascade test facility (task 3.3). The measurements were carried out for two transition control cases. The first one is roughness patch Ra=10 μm located on suction side at x/c=0.11 and 10 mm width. The second one are AJVGs with a hole diameter of D=0.4 mm, pitch angle ϕ=30° and skew angle θ=75°, spanwise distance (pitch) L/D=15. The detailed analysis of the steady and unsteady shock behaviour as well as the shock wave boundary layer interaction is based on:

- schlieren figures - characterization of the shock structure
- PIV measurements - detection of the shock position within the cascade and measurement of the shock wave boundary layer interaction region
- High Speed Shadowgraphy (HSS) - characterization of unsteady behaviour of the shock fluctuation

Numerical simulations for DLR cascade configuration were performed by 3 partners: RRD, Numeca and UAN. UAN performed simulations for basic flow configurations without transition control (then UAN left consortium). RRD investigated reference and transitional configurations with HYDRA code and k-ω Menter-SST model (including Langtry & Menter correlation if transition is taken into account). The roughness model which is applied in RRD flow solver is based on the ideas from Aupoix [1] and Eca & Hoekstra [2]. This model is artificially producing turbulence by tweaking k and ω equations in k-ω Menter-SST turbulence model. In case of AJVG configuration, two different approaches are applied. For the first, the aerofoil and the real AJVG geometries tested in DLR cascade are meshed using the unstructured grid generator BOXER. For the second, source terms are built on the suction side of the baseline structured mesh.

NUMECA investigated the capabilities of state-of-the-art turbulence models such as SST and of new promising model such as Explicit-Algebraic Reynolds Stress (EARSM) model in predicting shock-boundary layer interaction in laminar, turbulent, and transitional state. Using both models simulations were performed in fully turbulent mode and also coupled to a transport model for laminar-to-turbulent intermittency as originally described in Langtry (2006). NUMECA activity aimed at computing (Fine/Turbo) the DLR test section with roughness patch and investigating the possibilities of the turbulence and transitional models. The application of the S-BSL-EARSM turbulence model coupled to a laminar to turbulent transition module has been investigated with a roughness patch. The model has been adapted in order to be able to detect laminar to turbulent transition promoted by roughness elements. The effect of roughness patches onto the shock-boundary layer interaction was investigated by roughness elements included in the turbulence and

the transition models following the methodology developed in WP-2. Therefore, a modified solid wall boundary condition has been applied to ω equation, and a new correlation for laminar to turbulent transition promoted by roughness elements has been implemented.

Conclusions from WP-3 Partners

First of all, measurements for reference flow case in the single passage test section show very good agreement to the design requirements thus the flow structure on the transonic compressor profile (on suction side) is well reproduced. Reference case measurements prove that laminar shock wave boundary layer interaction leads to separation upstream of the main shock, whereas separation due to turbulent interaction just appears at the λ-foot. Experimental investigations of different boundary layer transition control devices show their influence on the shock in transonic conditions and possibility of separation bubble and shock wave oscillations reduction. However, the interaction is very sensitive to the upstream boundary layer and the aerodynamic performance can be easily decreased if tripping device is not properly applied. If the boundary layer was tripped just downstream of the leading edge (strip heights 0.1 and 0.4 mm) a thicker boundary layer is obtained, what increases λ-foot size and the shock wave pressure jump moves more upstream. Too thick boundary layer leads to the large separation zone downstream of shock wave, which in selected cases reaches even the trailing edge. As a consequence the wake width is much higher than without tripping device (Fig. 4).

Positive effect was obtained if roughness patch is properly located (Fig. 5). Within the investigated cases, the improvement of the wake parameters is the best for the roughness patch of Ra =12 μm located 21% of chord length. Oil flow visualization on the other hand shows that the boundary layer is not tripped upstream the shock along the whole span. The shock wave unsteadiness decreases for moderate treatment of boundary layer. In Fig. 6, the amplitude of the main shock wave oscillations for different measured flow cases is shown. The highest reduction of average shock oscillations was obtained for the roughness patch of Ra=10 μm at 11% of chord length.

Application of AJVGs as tripping device influences on boundary layer upstream of the shock wave and shows also promising potential for shock oscillation and pressure loss reduction.

Based on the experimental investigations at DLR cascade it is observed that lower losses appear for the fully turbulent SWBLI than for the laminar SWBLI. From the results of AJVGs as tripping device, one can state that AJVGs lead to a reduction of viscous losses on the blade suction side which is reflected by a significant reduction of the wake losses. This means, that only a small amount of additional losses is added to the viscous losses within the boundary layer by this control method. However, the shock structure is changed which leads to additional shock losses at the suction side region. Therefore, the sum of viscous and shock losses which is mainly influenced by these both effects is lower than for the laminar case but higher than for the fully turbulent case, where the transition is forced by the high turbulence intensity of the inflow. The measurements for the blade with roughness patch show a different impact of this boundary layer control method on the loss behaviour. There is only a small reduction of the viscous losses, in spite of a turbulent shock boundary layer interaction. Probably, it arises from the additional losses which are caused by the roughness patch. The measured boundary layer thickness at 30 % of the chord length is 50 % higher than at measurements of the fully turbulent and AJVG case. In the roughness patch case a higher amount of the loss reduction is caused by the changed shock structure in the passage which leads to a reduction of the shock losses compared to the laminar case.

Both experiments show that pressure losses can be reduced when tripping the boundary layer upstream the shock, however over tripping easily appears when incoming boundary layer is increased too much and causes massive increase in pressure losses.

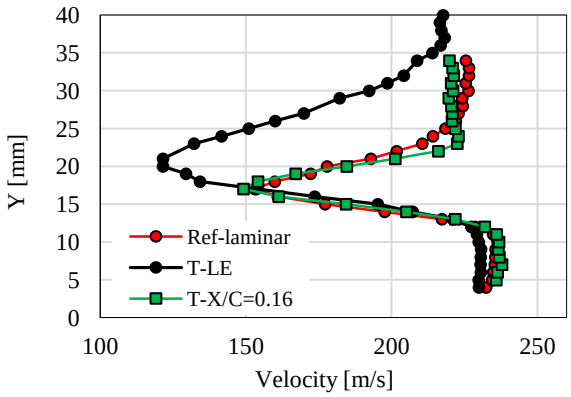

Fig. 4 Velocity (wake)

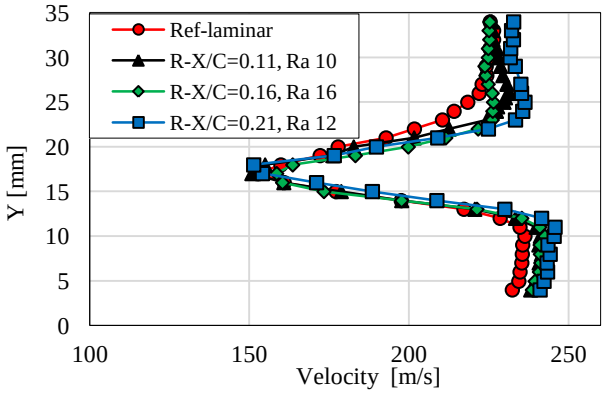

Fig. 5 Velocity (wake) –the best cases

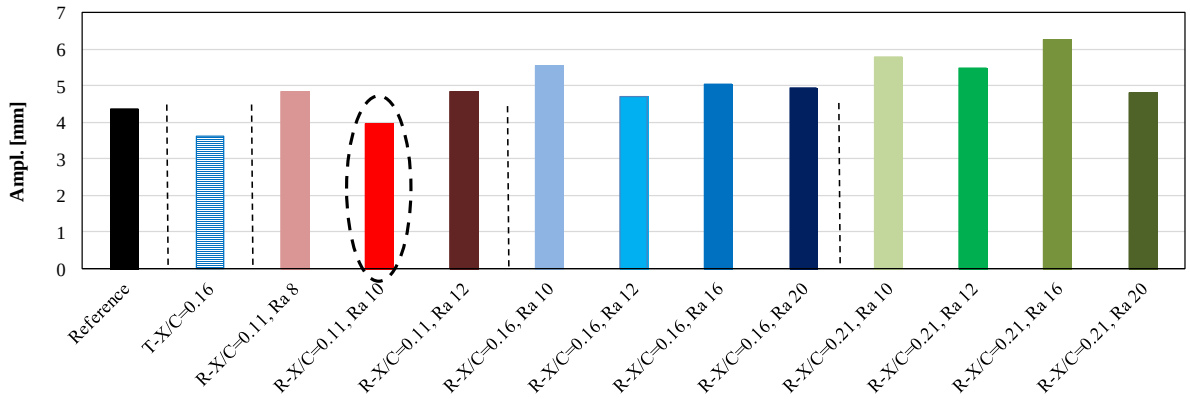

Fig. 6 Shock wave amplitude

URANS simulations done by RRD indicate that the roughness model which is implemented in Hydra solver is capable to achieve transition in a physical manor. However the range of different roughness heights in-between which successful boundary layer tripping appears is rather small and over tripping appears quickly. Compared to the reference, transitional simulations only small reduction in pressure losses were observed for simulations including roughness patch where all post processed parameters are showing that transition is not yet appearing upstream the shock. The reduction of pressure losses for the cases with roughness patch but not yet tripped boundary layer can be explained with slightly lower viscous losses due to a laminar shock boundary layer interaction with a laminar boundary layer with slightly more momentum compared to the reference laminar boundary layer. For the roughness height which is leading to a reasonable tripped boundary layer, the pressure loss is increased compared to the reference transitional simulation. Although the shock induced separation is considerably reduced for the tripped case, the pressure loss is lining up to the loss of the fully turbulent simulation.

Sensitivity study to the roughness height has been conducted by Numeca. Five different roughness heights have been investigated ranging from Ra=8 µm to Ra=20 µm. They all correspond to a transitionally roughness surface. Numerical results show that the pressure losses are a direct function of the height of the roughness element. Furthermore, a too big roughness height over-tripped the boundary layer upstream of the interaction and leads to bigger wake losses. All investigated roughness heights lead to increased pressure losses compared to the reference laminar interaction. Above a certain threshold value of about Ra=9 µm, the pressure losses are higher than the losses computed by the fully turbulent simulation.

Numerical simulations for both test configurations with AJVGs as tripping device are done by IMP PAN (single passage test section) and RRD (DLR cascade configuration). General conclusion is that the boundary layer tripping was achieved, but an increase of pressure losses is observed compared to the reference laminar SWBLIs.

Investigated cases and obtained experimental results allow to draw general conclusions. However, qualitative comparison of numerical results and experimental data for design condition show different effect on pressure losses when tripping the boundary layer (Fig. 7). Both measurements at IMP Pan in the single passage test section and at DLR in the cascade facility show that pressure losses can be reduced when proper tripping oft he boundary layer is achieved. However over-tripping easily appears, for e.g. only a small range of roughness heights are capable to reduce pressure losses compared tot he reference lamianr SWBLI.
In all performed numerical simulations at IMP Pan, RRD and Numeca tripping the boundary layer upstream the shock lead to increased pressure losses compared to the reference laminar cases. Those contradictory results between experiments and U/RANS simulations need further investigations and leaves the opened question: if U/RANS approach enables to obtain correct prediction of transition location and shock wave boundary layer interaction.

In respect to the unsteady behaviour due to SWBLI conclusions can be only derived from experimental investigations, since typical low frequency oscillations were not observed in URANS simulations. Experiments at IMP PAN did show that for certain cases including tripping devices the amplitude and the shock movement can be reduced compared to the laminar SWBLI. Results obtained at DLR cascade facility are not yet finally post processed and hence conclusions cannot yet be drawn.

Generally, improvement of flow parameters downstream of shock wave boundary layer interaction requires moderate treatment of the boundary layer upstream of the interaction. Overtripping (thicker boundary layer generated) appears in step manner and causes the deterioration of wake parameters and also sometimes increases the shock unsteadiness.

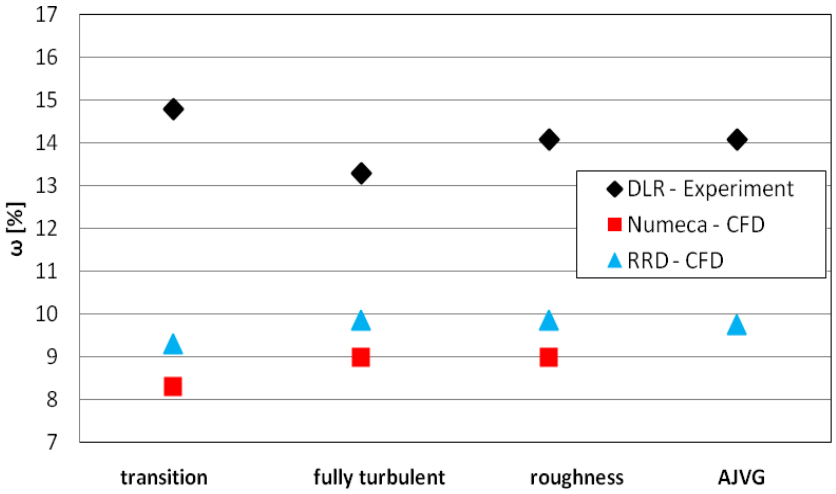

Fig. 7 Pressure losses in compressor cascade

Work Package 4 - Internal flows – turbine

Work package tasks – partnership and sharing of work

The Work package 4 is split into three tasks:

Task 4.1. Turbine blade suction side model
Task 4.2. Basic turbine cascade flow.
Task 4.3. Turbine cascade flow with transition control

The strong acceleration of the flow leads to a relaminarisation of the boundary layer and the interaction with shocks may cause separation. Investigations of the flow development on the blade

suction side were carried out in task 4.1. As described in the project DoW, there was planned to use in WP-4 the existing test section which was investigated in FP6 AITEB-2 project. However, RRD has decided to change the reference cascade and the new definition has been delivered finally. The new single passage test section was designed by means of numerical simulations at IMP PAN. The partners NUMECA and RRD were involved with computational simulations to support the test section design.

Originally, it was planned that the boundary layer tripping should be realised by means of the AJVG located downstream of the cooling holes. Due to the serious technological problem with the manufacturing of the appropriate configuration of the jet holes (skewed, inclined and small diameter 0.3 mm) the method of boundary layer tripping has been changed in the experimental investigations. Instead of AJVG the boundary layer transition control was realised by means of tripping step (height h=50 μm, h/δ=0.1). The following experimental techniques were applied at IMP PAN: static pressure along the lower wall and blade, schlieren visualization, oil visualization, shock oscillations measurements, velocity traverses measurements by means of LDA. Numerical investigations were carried out by means of Fine/Turbo NUMECA with EARSM turbulence model and transition model γ-Re_θ. AJVG location on the separation downstream of the shock wave were investigated numerically only (for single passage test section). Numerical simulations were also done by NUMECA with the local source terms for the coolant flow.

AJVG configuration for cascade measurements (DLR) were defined according to IMP PAN experience from AITEB-2 project and numerical simulations results. Manufacturing reasons had to be taken into account. A compromise of the location and inclination to the blade surface angle θ had to be found due to a strong profile curvature. Under consideration of all manufacturing reasons the diameter was set to 0.3 mm. This was also the criteria to choose the AJVG exit location. The boundary layer thickness was taken from numerical results from a cooled blade to determine the location. The AJVG location was set to x/c_{ax} = 54.4 %, angles α = 65° and θ = 35°.

The turbine blade was designed by RRD. To achieve relaminarization on the blade with film cooling, the two criteria from literature were applied. The first one is the acceleration parameter:

$$AC = \frac{\nu}{{u_e}^2} \cdot \frac{du_e}{ds}.$$

The acceleration should be higher than $3.5 \cdot 10^{-6}$. The second one is the Buri parameter, which takes into account the acceleration and the Reynolds number based on the momentum thickness:

$$Bu = {Re_\theta}^{\frac{5}{4}} \cdot AC$$

This parameter should be higher than 0.005. One coolant row was put into the Buri-region (stagnation flow) and the other one in the acceleration region. The pitch/c_{ax} ratio of the cascade is approximately 2. Mach number at the outlet Ma_{exit} was set to and Reynolds number $Re_{exit} \approx 1.1 \cdot 10^6$. The design was performed by means of a 2D cascade simulations with Mises and the TAU code.

The experimental investigations for cascade configuration within task 4.2 and task 4.3 were carried out in DLR test section in Goettingen. Following measurement techniques were applied: schlieren, pressure taps and total pressure wake traverses and hot wire measurements. To detect the transition location Infrared thermography and hot film measurements on a coolant blade were conducted. The coolant cavity pressure was set 5 % higher than the inlet pressure. The AJVG cavity pressure was the same as the main flow inlet pressure.

Numerical simulations were carried out by RRD, NUMECA and UAN. RRD applied two solvers: Fluent solver with k-ω SST turbulence model including the γ-Re_θ transition transport equation and CFX 14 with SAS-SST turbulence model and γ-Re_θ (unsteady simulations). NUMECA investigated the impact of AJVGs on the interaction between the oblique shock wave and the blade boundary layer along the DLR turbine cascade. The applicability of the S-BSL-EARSM turbulence model coupled to a laminar to turbulent transition module has been investigated with AJVGs. Furthermore, sensitivity study to AJVG mass flow rate and location should also be conducted. UAN numerical simulations (k-ω SST model) were focused on the influence of mesh refinement, turbulence intensity and turbulent length scale at the inlet, as well as values of transitional model constants on the flow structure, separation and kinetic energy losses. The work was performed for the basic cascade (without film cooling),

afterwards UAN terminated the participation TFAST project and the remaining work was taken over by NUMECA.

NUMECA carried out additional investigations, the influence of an uncertainty on the blade geometry of the DLR cascade, where the geometrical variation is achieved by modifying the trailing edge angle.

Conclusions from WP-4 Partners

The single passage investigations shown that the shock wave interacts with laminar boundary layer if no cooling is applied. Laminar type of interaction is indicated by the fact that at such relative low Mach number upstream of the shock (M=1.26) a very large λ-foot appears. Shock waves topology changes if cooling is applied and it is dependent on the blowing ratio.

Boundary layer separation is reduced in relation to the clean flow case (blade without film cooling). The separation size at such low Mach number upstream of the shock wave is very small and there is no particular difference in terms of its size between the investigated cooling blowing ratio.

Application of tripping device (strip) influence on the amplitude and RMS of shock oscillations decrease. In the investigated cases the RMS is lower about 10% and the amplitude is about 20÷30% lower in relation to the flow with laminar interaction. Separation size is significantly reduced (nearly fully attached) in relation to the case without tripping device. It is shown (Fig. 8) that in case of turbulent interaction at low Mach number upstream of the shock the λ-foot does not appears in the flow. Normal shock wave reaches the wall boundary layer. The disturbances upstream of the normal shock are the week Mach waves induced by the tripping strip.

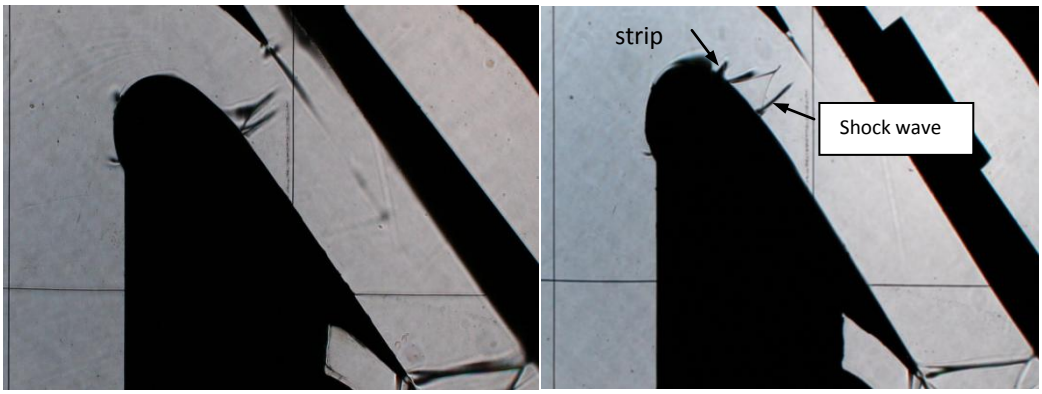

Fig. 8 Schlieren – no tripping device (left) and with strip (right)

Comparison of DLR cascade measurements, IMP PAN single passage test section and CFD results from NUMECA, RRD and UAN is shown in Fig.8. All results show good agreement at the pressure side and the acceleration zone. Downstream of the throat close to the interaction zone clear differences are revealed between all results. If the film cooling is applied the differences are much lower and the results are closer to each other (Fig.10).

The loss coefficients for the basic blade and the cooled one is shown in Fig. 11. The losses are calculated by the pressure ratios without considering the influence of coolant flow. It assumed that since the same temperature (no differences between main flow and coolant) at the inlet is applied, it does not have any effect on the enthalpy and can therefore be excluded from the evaluation. The results for the loss coefficients differ due to the different shock boundary layer interaction effect. In case of measurements, the coolant induces a slight decrease of losses with increasing mass flow ratio.

DLR measurements show an increase of losses in most of the investigated cases if boundary layer tripped by Air Jet Vortex Generators (Fig. 12). However, it was found that the separation

downstream of the shock wave is reduced.

Numerically predicted trend of loss coefficient are comparable to the experimental results. Noticeable is the loss peak at c_m = 0.13 %. The same effect is obtained by sensitivity study to AJVG location done by NUMECA. It is shown that AJVG can have a positive effect on the shock boundary layer interaction if they are located further upstream. Numerical results show that by reducing this interaction the downstream boundary layer remains partially laminar. The maximum extension of the recirculation zone has been reduced and the maximum thickness of the separation zone has also been reduced. It has a direct impact on the viscous forces acting on the blade surface and potentially on the heat transfer and the life-time of such a high pressure turbine blade.

RRD unsteady simulations results show decrease of shock wave oscillations, but higher total pressure losses.

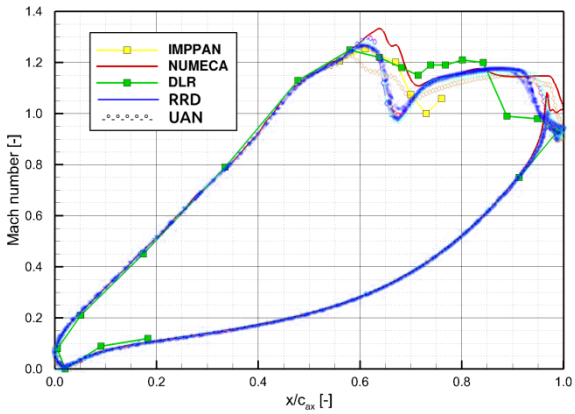

Fig. 9 Mach number distribution (Basic blade)

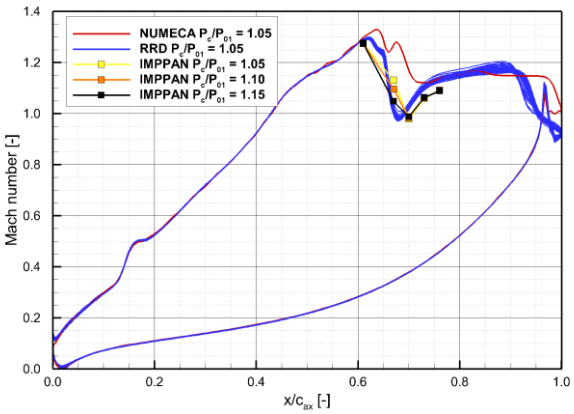

Fig. 10 Mach number distribution (Cooling blade)

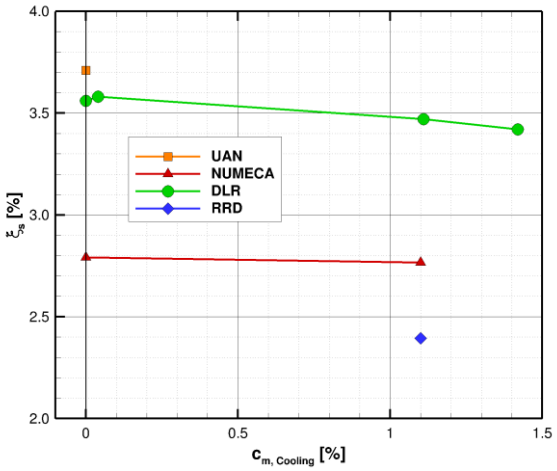

Fig. 11 Loss coefficient (cooling influence)

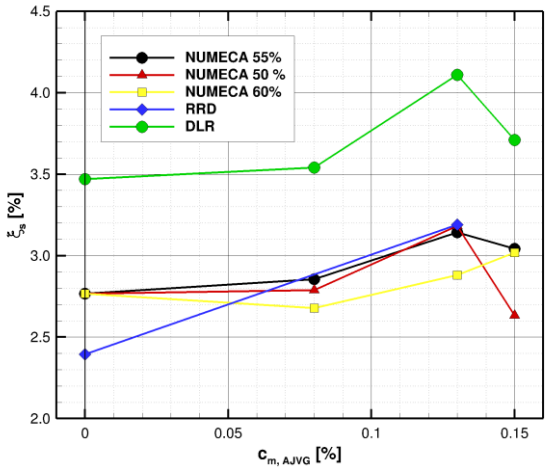

Fig. 12 Loss coefficient (cooling and AJVG influence)

Concerning the comparability of experiments and numerical simulations the following conclusions can be drawn:

- differences in Mach number distribution downstream of shock wave predicted and measured in DLR cascade
- onset and separation size differences

Experimental investigations leads to conclusion that the laminar boundary layer is very sensitive due to disturbances on the blade surface, especially due to surface roughness and due to the cooling/AJVG holes (even if no coolant or no jet flow).

Generally, improvement of flow parameters downstream of shock wave boundary layer interaction requires moderate treatment of the boundary layer upstream of the interaction, overtripping may appear in step manner and cause the deterioration of boundary layer parameters downstream of the interaction region.

Work Package 5 - External flows – wing

Work package tasks – partnership and sharing of work

Because of the high running cost of specialized large-scale transonic wind tunnels, using such facilities is not appropriate for upstream research programs such as TFAST. Therefore existing wind tunnels were used in the consortium. One of these is a transonic test section at UCAM where laminar and transitional profiles had been studied previously at Reynolds numbers up to 2 million (based on chord length). In the first task 5.1, a 2-D laminar airfoil was specifically designed by DAAV for transonic tests, and tested in the UCAM wind tunnel, with the aim to provide basic investigations of the transition location effects on shock-induced separation and unsteadiness for a relatively large number of parameters.

Then, tests in the larger wind tunnel of IoA were performed in task 5.2 which enabled investigation of a much larger aspect ratio profile. In this facility, it was possible to measure a whole force polar up to and including the buffet boundary. The experiment was conducted for natural boundary layer transition location as well as different methods of tripping. The task 5.2 included validation and improvement of various steady and scale resolving numerical methods, without and with transition control devices.

Finally, a purely CFD task 5.3 consisted of simulating a 3-D laminar wing, based on the experience gathered by CFD from simulations in tasks 5.2. The goal was to understand transition control effect on a real wing with a leading edge sweep and a tip vortex.

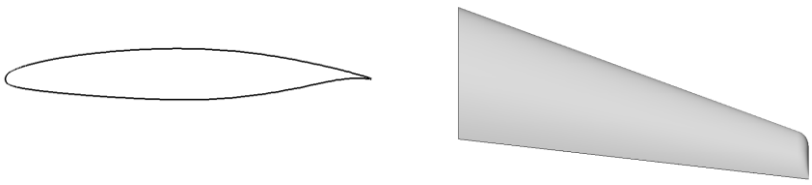

Fig. 13. Laminar wing

Table 5: WP-5 Experiments

Steady SBLI	[**UCAM / IoA / both**]
SBLI flow topology	Schlieren, PSP, pressure taps
Aerodynamic forces	Drag (LDV in wake), PSP CL (pressure taps), CD(aero. rake)
Buffet onset limit	Strain gauge
Unsteady (buffet)	
Shock structure	Oil flow, senflex sensors, PIV
Buffeting frequency, fluctuating pressure	High speed video Schlieren Kulites, Pressure taps
Buffeting amplitude	High-speed vid. Schlieren Schlieren, Kulites

DAAV has designed a laminar profile (termed V2C) used for task 5.1 and 5.2 and a laminar wing used for task 5.3 (Fig.13). The wing is based on the V2C profile with sweep and twist for a closer representativity of a real geometry. In both geometries, parabola method coupled with a boundary layer code were used to assess that laminarity was effective up to the shock (amplification factor and

wing root contamination below a given limit). The laminarity analysis has also provided guidelines for experimentalists in terms of maximum inlet turbulent intensity.

A wide range of measurement techniques were employed by IoA and UCAM, as summarized in the above table, to characterize turbulent, transitional and laminar SBLI. Prior to buffet onset (steady regime), the flow topology at SBLI, in particular the presence of a laminar or transitional separation bubble at shock foot, was evidenced by Schlieren visualization as well as surface pressure coefficient obtained with pressure taps or pressure sensitive painting. Pressure transducers signal integration on the surface and the wake allowed lift and drag coefficient to be measured, as well as their dependence on the tripping location. Buffeting occurring at unsteady SBLI was observed using high-speed video Schlieren visualization by UCAM, and IoA employed Kulites, unsteady pressure taps, strain gauge and senflex sensors. Oil flow visualizations were provided by both partners to determine transitional flow pattern and shock structure. Finally transition control effects were studied by UCAM using 2-D and 3-D trip dots as well as painting, and by IoA with carborundum of three different heights (0.1mm, 0.15mm, 0.26mm). The chord length of the model used at UCAM is c=100mm, with an aspect ratio of L/c=1 and test section height H=2c, whereas for IoA c=200mm, L/c=3 and H=3c. Due to smaller model and higher blockage, UCAM focused on moderate values of angle of attack, whereas IoA performed full polar measurements, but the complementarity of metrology employed, as shown in the above table, and the earlier availability of UCAM data has justified the importance of both test campaigns in task 5.1 and task 5.2 for the work-package achievements.

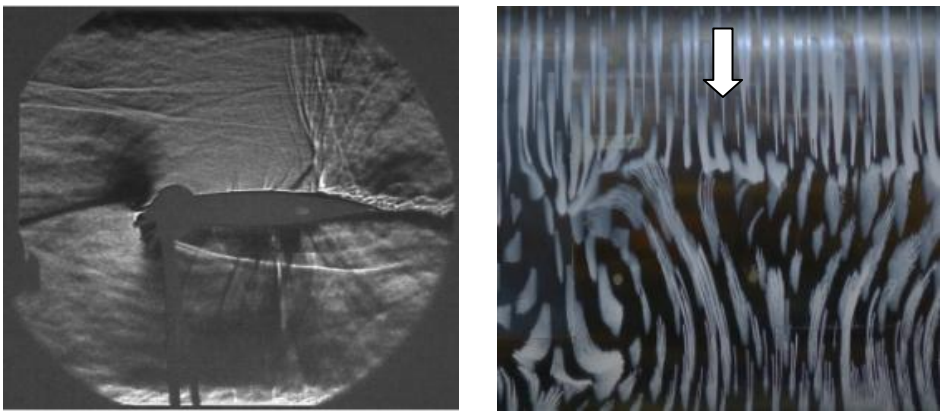

Fig. 14 Examples of experimental visualization. UCAM Schlieren for clean case (left), IoA oil flow (right)

Table 6: WP-5 Numerical study

	Laminar	Transitional (trip location)	Turbulent
WP5.2 Steady	[IoA / URMLS / DAAV / NUMECA / IMFT / LIV / all]		
Flow topology	k-w-γ-R_θ DNS (4°)		**RANS**
Aerodynamic forces	k-w-γ-R_θ / RANS + optimisation study + drag decomposition study		
Buffet onset limit	26 k-w-γ-R_θ URANS		40 DDES + 35 URANS / SST
WP5.2 Unsteady			
Shock structure **Buffeting frequency** **Pressure fluctuations** **Buffet amplitude**	URANS-k-w-γ-R_θ DNS (7°)	DNS (Trip 10%) Tripped ZDES k-w-γ-R_θ DDES, K-w-γ-R_θ URANS SST	OES k-ε, DDES Fully turbulent ZDES
WP5.3 Laminar wing			
Application of WP5.2 and WP5.3 findings to a «real life» configuration	EARSM LCTM K-w-γ-R_θ Tripped IDDES Tripped OES k-ε, K-w-γ-R_θ		

The table 6 summarizes numerical contributions for WP5.2 and WP5.3 for the three types of interactions. This includes implementation, calibration and application of the k-w-γ-R_θ transition model (IoA, LIV, IMFT, NUMECA) for laminar and transitional SBLI, for which three direct simulations (DNS) were also performed by URMLS thus providing additional reference data for models validation. The study of transition location effect was covered by IoA and IMFT to determine the optimal tripping location which yields best aerodynamic performances (in terms of lift-over-drag ratio). Sensitivity to the nature of tripping was also investigated by IoA (using vortex generators of heights similar to carborundum height used in IoA experiment and located at 0%, 6%, 15%, 30% and 60% chord) and LIV (using CoC1 as well as air jet vortex generators). The determination of buffet onset limit (in terms of critical Mach M_∞ and flow incidence α) was carried out by URMLS (URANS and DDES), IMFT and LIV (URANS) who performed parametric study in the (M_∞, α) domain. Finally, several partners (DAAV, URMLS, IMFT, LIV) performed scale-resolving simulations ((I)DDES, OES) of buffet using various mesh resolutions and underlying RANS turbulence models.

Conclusions from WP-5 Partners

Steady SBLI for M=0.7, α=4°

The presence of a separation bubble at shock foot for laminar or transitional SBLI yields the presence of a plateau in pressure coefficient distribution, with laminar (resp. turbulent) separation bubble characterized by a strong rear (resp. front) foot of the λ-shock, seen on experimental and numerical results shown in Fig. 15. Plots in black (resp. red) are data for the open-air (resp. in-tunnel) configurations. The analysis enabled to distinguish laminar interaction from mere boundary layer (BL) thickness effects of turbulent interaction, even for BL tripped just before shock. The importance of transition modeling (approaches providing smooth evolution of intermittency γ rather than simple Heaviside-function used for numerical tripping) proved essential for this type of flows.

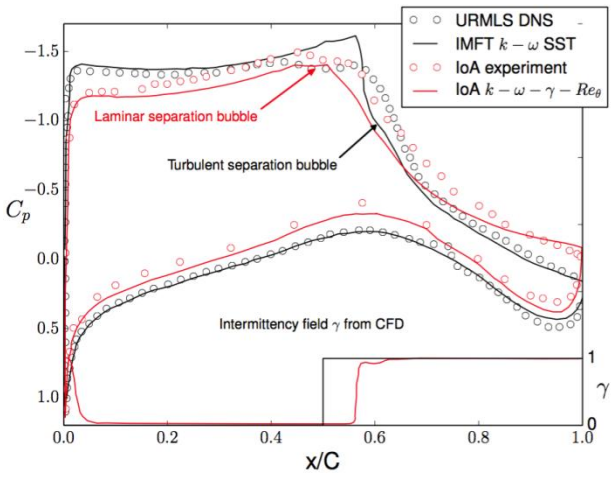

Fig. 15 Pressure coefficient distribution

Dependency of aerodynamic coefficients on tripping location

Drag coefficient and lift-over-drag ratio, as function of tripping location, are shown in Fig. 16, from IoA (experimental and numerical study) and IMFT. It was generally observed that increased laminarity (i.e. tripping closer to shock) expectedly yielded lower friction drag, but resulted in strong shock, thus higher wave drag. The maximum lift-over-drag ratio therefore is obtained for a tripping location somewhere between leading edge and shock position, commonly found at around 30% chord length for the present case.

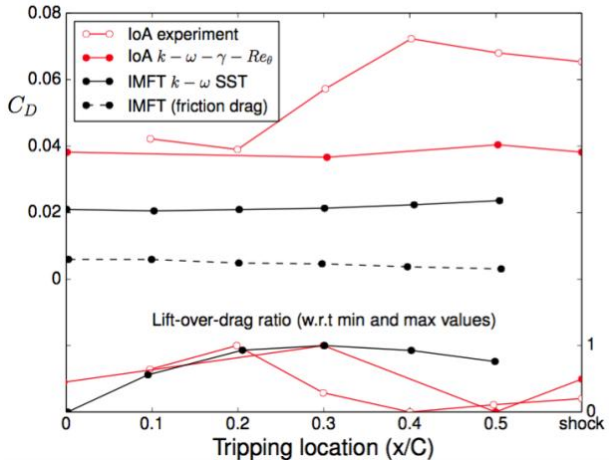

Fig. 16 Drag coefficient and lift-over-drag ratio

Buffet limit

The experimental detection of buffet onset when varying the Mach number or the flow incidence was performed by IoA using strain gauge. The study was also numerically carried out using several URANS models as well as DDES by LIV, IMFT and URMLS. Buffet map was determined by Mach/Incidence parametric study requiring between 25 and 40 simulations to be carried out for each approach. The study (Fig.17) reveals a good agreement between SST URANS and DDES methods, whereas the k-w-γ-R_θ predicts an earlier onset with respect to incidence.

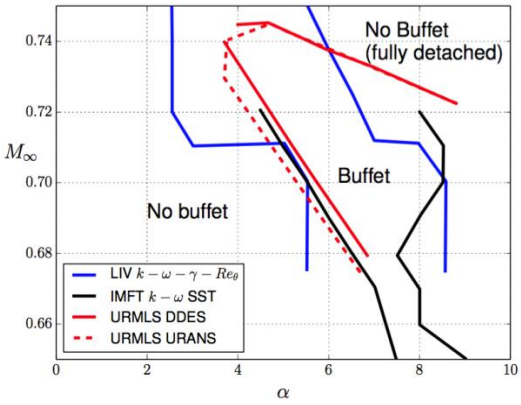

Fig. 17 Buffet map

Unsteady SBLI with buffet for Mach=0.7 and α=7°

The full buffet regime was the object of several DDES and DNS at IMFT, URMLS, LIV and DAAV. The investigation focused on shock amplitude, lift and drag oscillations amplitude and frequency, and pressure fluctuations downstream of the shock. Only transitional or turbulent interactions were covered by DDES (Fig.18), with a strong dependency of shock oscillation amplitude and extreme shock position on turbulence model and grid, although a Strouhal number associated to buffeting instability was commonly found to be around St=0.1 based on chord length. The above plot presents the drag coefficient history, provided by the DDES of UMLRS and DAAV and the k-ε OES of IMFT. Laminar buffeting study was covered by IoA experiment and URMLS DNS that both reported very low oscillation amplitude of shock, lift and drag coefficients, suggesting an opposite trend to turbulent buffet.

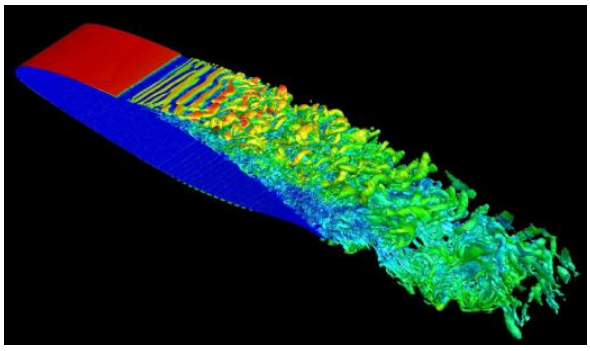

Fig. 18 Visualisation of Q criteria (DAAV DDES)

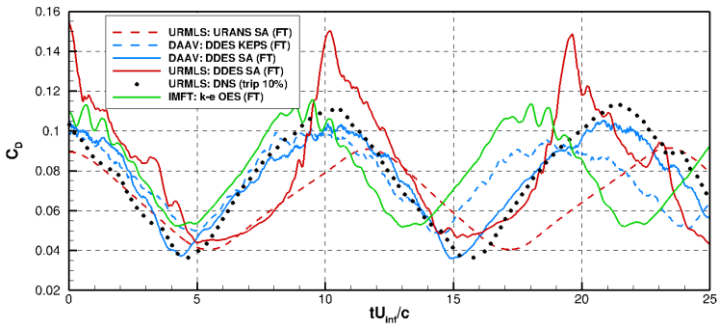

Fig. 19 Drag coefficient history

Natural and transitional SBLI on the laminar wing

Starting from DAAV guidelines (M_∞, α) values for buffet onset, partners involved performed URANS with transition modeling (k-w-γ-R_θ) (IMFT, LIV, NUMECA) and scale resolving simulations (LIV: IDDES, IMFT: k-ω OES), with fine-tuning of the tripping position to account for models influence and/or the Mach number to correct the sweep effect, with the aim to detect buffet. Simulations from LIV and IMFT reveals milder shock oscillation than for the previous V2C case, and IMFT investigated the span-wise dependency of buffeting frequency (due to the local chord-length based Reynolds number being different). LIV performed additional simulations to verify the effectiveness of VGs, AJVGs and flaps to suppress buffet.

Main TFAST Project achievements

It is known that designing an experiment in transonic and transitional conditions is a difficult task, which had to be rediscovered, on the basis of the experiments performed in the sixties. This took time, but was finally successful with configurations consistent with the qualitative descriptions of obtained in the past. Methods like PSP and TSP were successfully used to give a rapid and global view of the flows at the wall. For more detailed information, a particular effort had to be put on particle methods. Despite severe limitations related to seeding and space resolution problems, they bring new quantitative data, useful for the validation of the numerical simulations and for the physical description of the flow. Fluctuating fields could be obtained only with particular flow and optical settings. It is clear that such methods, although of unique potential, have still to be complemented for unsteadiness measurements by classical methods like hot-wire anemometry which in this case remains a simple, accurate and reliable tool.

Most of the work of WP-1 was done in 2-D situations, but the mechanisms put in evidence are believed to be general enough to be used as a guide for more complex situations. Some points have been clarified. During the project, the different partners have used several Mach and unit Reynolds

numbers. Possible ways to compare the different results and their mutual consistency are now clearer. Similarly, the point of the onset of (2-D) separation has been documented.

Conclusions can be drawn about the numerical methods. Methods based on stability analysis proved to be insightful. Moreover, the low Reynolds number flows studied by TFAST are attractive for methods like DNS and LES which proved to be efficient. Their efficiency has been shown during the project, including wall perturbations. Of course their cost is still such that it is difficult to use them in the design routines for industry, but their potential is real and present.

A major conclusion is probably that these transitional flows are very sensitive to the level of external background fluctuations, so that their organization (size of the separated zone, spreading of the pressure distribution, etc…) depends critically on the nature of the perturbation: the mean flow is directly influenced by them. This means that the external level of background turbulence, or the fluctuations introduced by wall perturbations are major parameters for the determination of the mean field and of the low Reynolds number turbulence formed in and downstream of the interaction. These points have been documented in the TFAST experimental results database.

A second conclusion is relative to the low frequency unsteadiness which is found in the interaction. It seems directly related to the transitional mechanism along the interaction. There is still some controversy on their dimensionless values between numerical and experimental results, but similar space-time properties and amplitudes have been observed.

The main achievement of WP-2 is to produce a comprehensive database for transitional SBLIs under the influence of transition trips and flow control. Thus, the existing knowledge of transition tripping in high-speed flows (at practical Reynolds numbers) was extended comprehensively. A comparison of tripped and un-tripped configurations also revealed that in many cases it is not detrimental (even beneficial) to allow the shock wave 'to do the work' and promote transition in the interaction zone. These findings are only valid for interactions on flat surfaces which was the scope of this work package. Nevertheless, this unexpected result is a valuable contribution to the knowledge of compressible flow.

Investigated turbomachinery configurations (WP-3 and WP-4) show that improvement of flow parameters downstream of the shock wave boundary layer interaction, separation and shock oscillations reduction, requires moderate treatment of the boundary layer upstream of the interaction. Overtripping (thicker boundary layer generated) appears in rapid manner and causes the deterioration of wake parameters and also sometimes increases the shock unsteadiness.

A considerable amount of experimental and numerical data were produced to characterize tripping location influence on SBLI prior, at, and beyond buffeting onset, although no unique conclusion could be drawn due to 1/ heterogeneity of results and flow conditions, 2/ blockage effect in both tunnels that influenced buffet onset and was not (as intended) always been accounted for in simulations, 3/ challenges inherent to experiments with laminarity (influence of model roughness and manufacturing, intrusive metrology), 4/ prevalence of fully turbulent methods in buffet simulations and 5/ grid and models dependency, mostly for transitional buffet simulations.

Nonetheless, the following lessons could be formulated:

- The laminar flow benefit (lower friction drag and enhanced lift due to the shock being pushed backwards) could be reduced when wave drag becomes comparatively significant, as evidenced both experimentally and numerically, showing wave drag could increase for laminar or transitional SBLI.
- Experimental studies could not characterize a strong buffet onset dependency on tripping. At full buffet regime, experimental observations (IoA) and DNS results (URMLS) tend to suggest buffeting frequency and aerodynamic fluctuations are considerably reduced for transitional or laminar SBLI, which would tend towards the conclusion that unsteady laminar interaction is not detrimental and does not need to be avoided.

Physical models for laminar and transitional SBLI are upgraded. Several partners have implemented transition models (such as the k-w-γ-R_θ model) with calibration of the correlation

function and testing on both 2-D and 3-D reference cases. The intermittency provided by these methods proved essential to predict laminar separation bubble at shock foot, as well as a realistic flow tripping when tripping devices are numerically represented or modeled, therefore demonstrating readiness of such methods for industrial use. Moreover, unsteady configurations were the object of a large number of scale resolving simulations ((I)DDES and OES), that, in the framework of the TFAST project, proved very useful in providing information on coupling mechanisms at the origin of the buffeting phenomenon.